Nanostructures

Micrometer-Sized Hexagonal Tubes Self-Assembled by a Cyclic Peptide in a Liquid Crystal**

Steve Leclair, Pierre Baillargeon, Rachid Skouta, David Gauthier, Yue Zhao, and Yves L. Dory**

Self-assembly of cyclic peptides is an attractive strategy for making hollow tubular structures.[1–4] Stacking of ring-shaped molecules of flat conformation can be stabilized by intermolecular hydrogen bonds formed between the amide groups. Cyclic peptides of rationally designed chemical structures can form nanotubes of different internal diameters and structures, which may find applications in biology and materials sciences.[2,5,6] Generally, the self-assembly process occurs in solution, is often triggered by a change in solubility of the peptide in organic solvents, and results in crystals organized by nanotubes. Herein, we report on the observation of self-assembled structures of a cyclic peptide in a nematic liquid crystal (LC). Hexagonal hollow tubes that have diameters in the order of micrometers and reaching several millimetres in length were observed. Strong experimental evidence suggests the occurrence of a hierarchical and self-similar-structured self-assembly of the cyclic peptide. That is, individual molecules of hexagonal conformation stack up into hexagonal nanotubes, which then self-organize into larger aggregates with the same appearance. Each molecule provides both intra- and intertube H bonding that ensure the molecular stacking within and the packing of nanotubes. To the best of our knowledge, this is the first work exploring the use of liquid crystals for the self-assembly of cyclic peptides, and the results show the surprising impact of the liquid crystalline medium.

Previous work showed that the lipophilic macrolactam cyclo-$(NHCH_2CH{=}CHCH_2CO)_3$ (*E* olefin) is soluble in ethanol and can be crystallized by diffusion of diethyl ether.[4] The crystal structure determined by X-ray crystallography shows the stacking of macrocycles, which have a

[*] S. Leclair, Prof. Y. Zhao
Laboratoire de polymères et cristaux liquides
Département de Chimie
Université de Sherbrooke
Sherbrooke, Qc, J1K 2R1 (Canada)
Fax: (+1) 819-821-8017
E-mail: yue.zhao@usherbrooke.ca

P. Baillargeon, R. Skouta, D. Gauthier, Prof. Y. L. Dory
Laboratoire de Synthèse Supramoléculaire
Département de Chimie
Université de Sherbrooke
Sherbrooke, Qc, J1K 2R1 (Canada)
Fax: (+1) 819-821-8017
E-mail: yves.dory@usherbrooke.ca

[**] This work was supported by NSERC Canada and FQRNT Québec. We thank Drs. S. Jandl and G. Riou, Sherbrooke, for the Raman microspectroscopic measurements.

Supporting information for this article is available on the WWW under http://www.angewandte.org or from the author.

 DOI: 10.1002/anie.200352259

rectangular shape due to one β turn, and the arrangement of the nanotubes into an orthorhombic cell structure. In the study presented herein, the same macrolactam was dissolved in a nematic LC (BL006 from Merck), which is an eutectic mixture mainly composed of biphenyl compounds and has a nematic–isotropic transition at $T_{ni} = 115\,^{\circ}C$. The purpose was to know how the LC medium, which is a fluid but has molecular order, could affect the self-assembly. To prepare the mixture, both compounds were dissolved in ethanol/chloroform 40:60 (w/w), and the solvent was removed. The mixture was flow-filled (at 120 °C) into a glass cell, with a gap of 10 μm. The self-assembly was triggered by a change in temperature; by cooling the mixture from the isotropic phase, in which the peptide is soluble in the LC, to lower temperatures results in aggregation. At a low peptide concentration of 0.5–2 % w/w, the aggregation was observed only in the nematic phase, that is, below 115 °C. Thermally induced self-assembly is a common method used to prepare organogels[7] and liquid-crystal gels.[8]

When the mixture was cooled very slowly, long tube-like aggregates were formed, as is seen from the photomicrograph for a mixture containing 0.5 % peptide and cooled at $0.1\,^{\circ}C\,min^{-1}$ (Figure 1 a). The tubes may be as long as several millimetres and have a diameter of a couple of micrometers. Analyses under crossed polarizers revealed that these tubes retain the LC inside. By dipping the cell in hexane, the LC can be removed slowly. After the cell was opened and dried, the tubes remained intact on the surface of the glass plates. A field emission gun scanning electron microscope was used to examine the tubes. Surprisingly, tubes of various diameters have a hexagonal form (Figure 1 b). Figure 1 c shows a broken tube of larger magnification. The cavity inside is visible and the surface of the tube is smooth. Figure 1 d shows the end of a naturally terminated tube, which is closed but remains highly porous. A very slow aggregation process is key to the formation of large and long tubes, which can also be obtained by isothermally annealing the mixture at a temperature below but close to T_{ni}. Smaller and shorter tubes are formed with an increase in the cooling rate or a decrease in the isothermal-annealing temperature. The striking features in Figure 1 (large cavity and hexagonal form at various diameters) are reminiscent of the concept of self-similar structure, which is used to describe loose and open-structured colloidal aggregates growing with the same appearance at any level of magnification.[9] In what follows, we present a computer modeling and Raman and infrared microspectroscopic analysis that points to a self-assembly mechanism for the observed amplification of the hexagonal form and the hollow structure of the tubes.

The rectangular nanotubes formed in the crystal cannot organize into hexagonal structures that provide the basis for a self-similar-structured growth in diameter of the observed tubular aggregate. We used computer modeling (6.31G* basis set and MM2 force field) to look for possible ways of aggregation for the cyclic peptide to form hexagonal objects. Using ab initio, we found three stable C_3 symmetric conformers[10] with energies of −0.22, 2.56 and 5.09 $kcal\,mol^{-1}$ relative to the crystal conformer.[4] Of the three conformations, the most stable one is unsuitable for stacking through

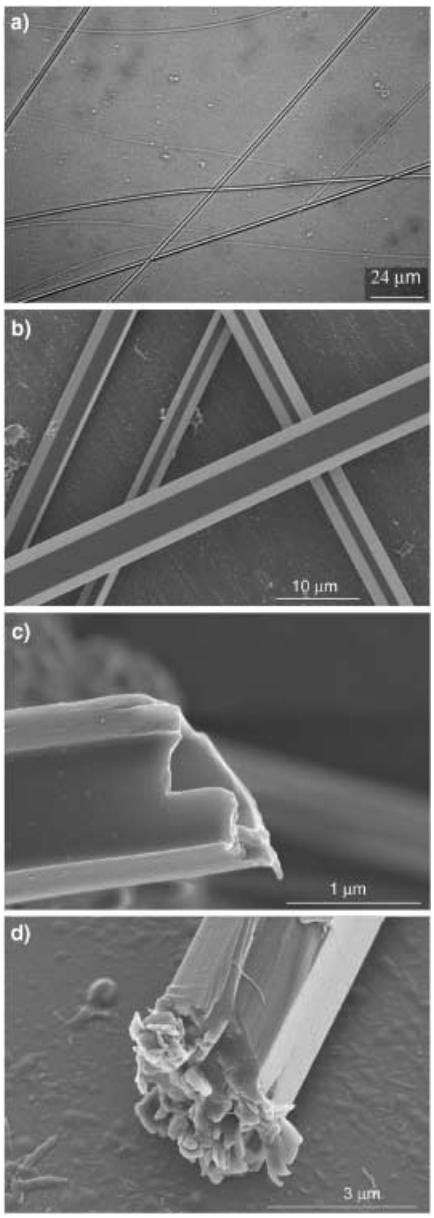

Figure 1. Images of the aggregates: a) Optical microscope; b) to d) scanning electron microscope.

hydrogen bonds, while the stacking of two units of the second stable conformer produced a dimer 12.48 $kcal\,mol^{-1}$ more energetic than the crystal dimer. On the other hand, the less stable conformer gave a parallel dimeric stack and an antiparallel stack (β-sheet description) with relative energies of 5.70 $kcal\,mol^{-1}$ and 6.38 $kcal\,mol^{-1}$, respectively. The lowest-energy dimer, shown in Figure 2 a, has roughly the shape of a hexagonal prism, with a crown of three amide carbonyls at one end, and a crown of three amide NHs at the other end. We then used MM2 force field, which was found to be sufficiently accurate to reproduce the 6.31G* results, to model the stacking and packing of the parallel dimeric stacks. Such hexagonal units can indeed stack on top of each other with the help of three hydrogen bonds to generate a first-generation hexagonal tube that has six alternating lipophilic and hydrophilic faces (Figure 2 b). The polar faces with

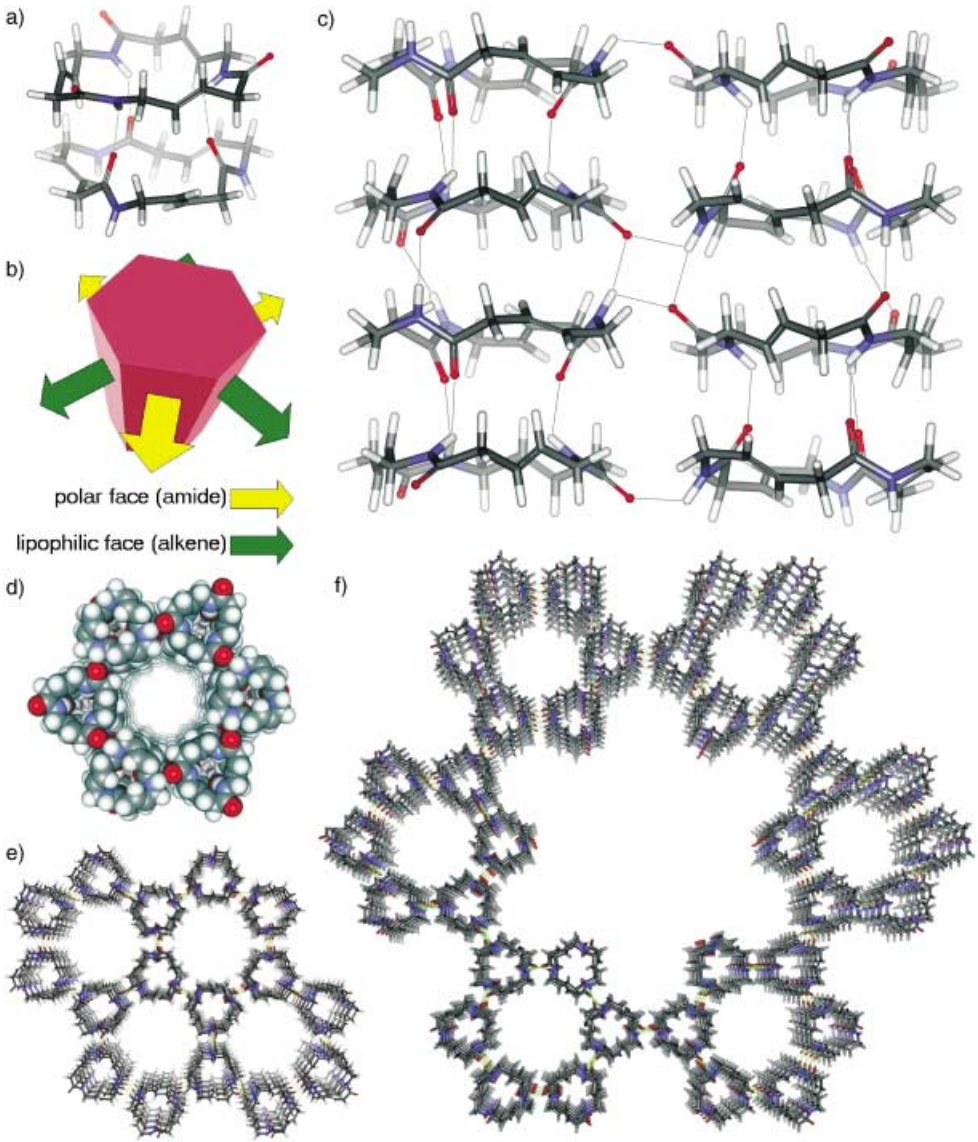

Figure 2. Hierarchical assembly to hollow macrotubes. a) Lowest-energy dimer with three intercycle hydrogen bonds. b) Schematic illustration of the first generation nanotube with intratube hydrogen bonds. c) Lowest-energy packing of two tetramers with intercycle and intertube hydrogen bonds. d) Lowest energy 48-mer as a second generation tube made of a hexagonal pack of six first-generation octameric nanotubes. e) Possible growth by packing of first generation nanotubes. f) Possible growth by packing of second generation tubes. O red, N blue, C gray, H white, H bond green line.

amides can establish interstack hydrogen bonds with neighboring tubes, whereas the hydrophobic faces with alkenes could only interact through van der Waals interactions. Calculations revealed that the most stable way for side-by-side packing of the first generation nanotubes is to have each nanotube with its gross dipole antiparallel to the neighbors. Figure 2c depicts the lowest energy packing of two tetramers showing the nature and orientation of the inter-cycle and intertube hydrogen bonds.

A thorough investigation was further carried out on various oligomeric aggregates that have 2, 4, 6, 8, 12, 24, 36, and 48 units to determine which type of assembly would predominate at each stage. Calculations yielded clues and interesting concepts as regards to the way mesoscopic hexagonal tubes might have formed in liquid crystals.[11] Although stacking of the rectangular crystal conformer is favored up to 12 units, for 24 units the packing of three hexagonal octameric first-generation tubes was preferred. After that point, hexagonal second-generation tubes made of six first-generation tubes become the rule, such as the 48-unit aggregate shown in Figure 2d. This second-generation tube keeps a hexagonal form like its precursor, but the diameter of the interior cavity increases to 10 Å. In contrast with the compact crystal packing that involves only weak van der Waals interactions,[4] the second generation hollow tubular structures may develop stabilizing van der Waals interactions with the lipophilic LC[6] in addition to the hydrogen bonding. In other words, the LC host could act as an active medium sampling C_3 symmetric units[12] and promoting the formation and growth of the hollow structures. From the second generation nanotube, further assembly into the observed micrometer-sized aggregates, while retaining the hexagonal form, may proceed through two mechanisms as illustrated in Figure 2. The first is a uniform packing (Figure 2e), which, however, will give rise to tubes with no large cavities. The second is a self-similar-structured growth. That is, the assembly of six second-generation tubes in the same way as the packing of six first-generation nanotubes will lead to an amplified hexagonal tubular structure with an increased internal cavity (30 Å) (Figure 2f), and the process of assembling the third and higher-generation tubes may go on to end up with the micrometer-scale tubes with a large interior cavity. We cannot rule out the first mechanism, but the observed hexagonal hollow tubes should come from a mechanism close to the second one. What actually happens is probably a combination of both mechanisms, which largely depends on experimental variables such as the cooling rate and the concentration of peptide. We observed that after the tubes were discernible on optical microscope, they grew in

length over time while their diameters remained unchanged. This suggests that at the earliest stage of aggregation or crystallization, short nanotubes of various generations may self-organize into a sort of stable two-dimensional hexagonal aggregate, which then serves as the seed for further longitudinal growth of the tube.

The key points of the above modeling analysis are that the observed large hexagonal tubes would be built up from nanotubes through a hierarchical and self-similar-structured process, and that both intratube and intertube hydrogen bonding should be involved in the stacking of the cyclic molecules, which form the first generation nanotubes, and the packing of the nanotubes, which ultimately results in the microtubes. Having no access to microbeam X-ray diffraction facility, we used Raman microspectroscopy to probe the structure of the tubes. As is depicted in Figure 3a, the excitation laser beam ($\lambda = 633$ nm), which had a diameter of about 1.5 μm, was focused right on a tube (diameter ≈ 2.5 μm) stayed on the surface of the substrate after removal of the LC. The polarization of the laser beam, which propagated along the *y*-axis of the coordinate system, was set to be parallel and perpendicular, respectively, to the long axis of the tube, that is, along the *z* and *x* axis, and in each case polarized emissions were recorded with the polarization of the analyzer being parallel and perpendicular to the laser polarization, thus yielding Raman spectra of $\boldsymbol{I}_{zz}$, $\boldsymbol{I}_{zx}$, $\boldsymbol{I}_{xx}$ and $\boldsymbol{I}_{xz}$ (the first letter in the subscript indicates the polarization direction of the laser and the second letter is for the polarization of the analyzer). The amide band in the 1600–1700 cm^{-1} region, from the C=O stretching mode, has an anisotropic Raman tensor and can be used to characterize the orientation of hydrogen bonds formed between amide groups in proteins or peptides.[13,14] It is worth noting that in Figure 3a, $\boldsymbol{I}_{xz}$ differs only very slightly from $\boldsymbol{I}_{zx}$, which ensures that the same portion of the tube was excited by the laser during the measurements. Several observations can be made by comparing $\boldsymbol{I}_{zz}$ and $\boldsymbol{I}_{xx}$. First, two C=O bands (amide I) appear at 1664 and 1634 cm^{-1}, thus indicating that there are two types of hydrogen bonds formed between C=O and N–H groups. The hydrogen bonds associated with the 1664 cm^{-1} band are found both along the tube ($\boldsymbol{I}_{zz}$) and normal to the tube ($\boldsymbol{I}_{xx}$). By contrast, the hydrogen bonds associated with the 1634 cm^{-1} band are almost exclusively aligned along the tube, as is indicated by the ratio of the intensities of the bands, $I_{zz}/I_{xx} \approx 10$. Second, the broad band centered at 1424 cm^{-1} arises from CH and CH_2 deformation[13] of the cyclic peptide. The main component of their Raman tensor apparently lies in the plane of the cycle, which leads to more intense emission of $\boldsymbol{I}_{xx}$ than $\boldsymbol{I}_{zz}$ ($I_{xx}/I_{zz} \approx 4$). Third, The band at 1590 cm^{-1}, which is absent for the crystal formed from solution, is assigned to the liquid crystal locked inside the tube. Indeed, polarizing optical microscope observation shows that the LC may be trapped in some tubes or sections after removal of the LC with hexane. The pure LC displays an intense Raman band at 1605 cm^{-1} (in-plane stretching mode of phenyl rings) that has a highly uniaxial Raman tensor.[15] A shift of this band to lower frequency in the tube could occur owing to interactions with the peptide molecules. Since the LC contains mainly biphenyl compounds, the different emissions of $\boldsymbol{I}_{xx}$ and $\boldsymbol{I}_{zz}$ ($I_{zz}/I_{xx} \approx 4$) indicate that the encapsulated LC molecules are aligned along to the tube.

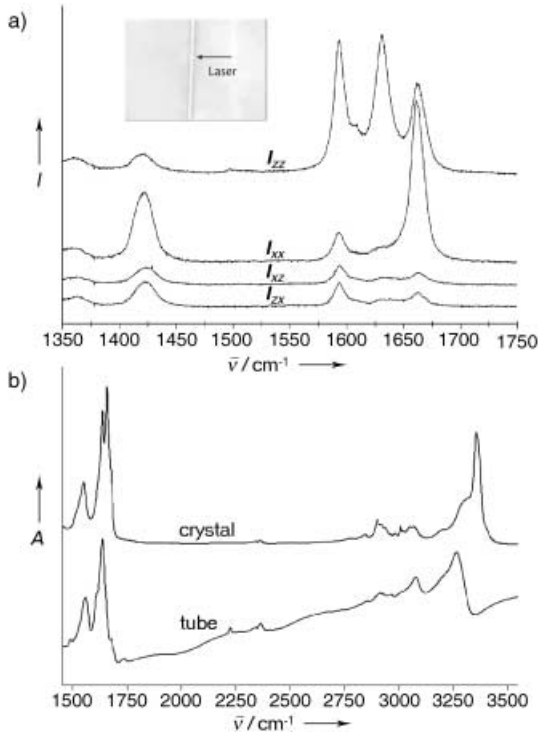

Figure 3. Raman and infrared spectroscopy of the tubes. a) Polarized Raman spectra in the 1350–1750 cm^{-1} region of a self-assembled tube (inset photo). The tube was positioned along the *z* axis and the incident laser beam was directed along the *y*-axis of the coordinate system (*I*: Raman intensity). b) Infrared spectra for the tubes self-assembled in the liquid crystal and the crystal (*A* = absorbance).

The polarized Raman microspectroscopic measurements strongly support the key features emerged from the modeling analyses, which include the stacking of the cyclic molecules along the tube direction and the sharing of intercycle (intratube) and intertube hydrogen bonds. On the one hand, the basic model in Figure 2c reveals indeed two types of hydrogen bonds. The first, formed between one C=O and one N–H, is only intercycle hydrogen bond, which would correspond to the 1634 cm^{-1} band observed only along the tube (Figure 3a). The second involves two C=O and two N–H groups, thus forming four hydrogen bonds (each O atom interacts with two H atoms and vice versa). These are both intercycle and intertube hydrogen bonds, which should be observed in the two directions (along and perpendicular to the tube). On the other hand, the model implies different conformations of the peptide molecules in the tubes and in the crystal, which affects the way they establish and use the hydrogen bonds for self-assembly. This also is qualitatively supported by the microspectroscopic analyses. The Raman spectra recorded with the crystal obtained from solution show the main amide I band shifted to 1680 cm^{-1}, with three other bands at 1669, 1643 and 1630 cm^{-1}. We also used infrared microspectroscopy to confirm the differences between the microtubes and the crystal. Their infrared spectra in the 1500–3500 cm^{-1} region are shown in Figure 3b. For the spectrum of tubes, the incident beam of about 100 μm was directed to an

area containing several tubes laid randomly on the surface of a CaF_2 window. The major differences can be seen from the hydrogen-bonded N–H stretching bands around the 3200–3300 cm^{-1} region. For the crystal two bands appear at 3358 and 3319 cm^{-1}, while for the tubes they are shifted by about 100 cm^{-1}, to 3266 and 3218 cm^{-1}, respectively. Similar spectral changes can be noticed for the two C=O bands, which shift from 1656 and 1637 cm^{-1} for the crystal, to 1637 and 1614 cm^{-1}, respectively, for the tubes. These results indicate that the tubes formed in the LC have different structures. As a matter of fact, in addition to the hexagonal form and opened structure, the tubes melt at about 203 °C, while no melting could be observed for the crystal before thermal decomposition at about 212 °C.

The formation of micrometer-sized hexagonal hollow tubes, an amplification of the hexagonal conformation of the molecule, is a spectacular manifestation of the effect of the medium on the way the peptide molecules use hydrogen bonding to self-assemble. The modeling and spectroscopic characterization results discussed above show that this is a case of both conformational and packing polymorphism. With respect to the dense crystal structure obtained from solution, the hexagonal hollow structure certainly is not the thermodynamically most stable organization, but is kinetically the most favorable outcome of a slow aggregation process occurred in the nematic LC. As mentioned above, the filling of the LC fluid inside the cavity and the interaction of the LC molecules with the peptide at the interface may stabilize the building of these large hollow tubes. More studies of self-assembly of cyclic peptide in liquid crystals are under way in our laboratories.

Experimental Section

Cooling of the peptide/LC mixture from the isotropic phase was controlled by using the hot stage of a microscope. A Leitz DMR-P polarizing optical microscope was used to examine the tubes in the LC and also after removal of the LC in hexane. The tubes remained on the surface of the substrate were studied by using a Hitachi S-4700 FEG scanning electron microscope as well as Raman and infrared microspectroscopy. Raman spectra of the tubes were recorded on a Jobin Yvon HR800 microspectrophotometer by using the 633 nm excitation from a He–Ne laser. The laser beam, passing through a 100× objective, was positioned on the tube, and the backscattering (360°) was collected. The beam intensity on the tube was about 6.4 mW. The four polarized spectra in Figure 3a were obtained by changing the polarizations of the laser and the analyzer without rotating the tube. The spectral recording was made on several places of the tube, and the results were very much reproducible. The infrared spectra were obtained by using a Nicolet Nic Plan microscope (15×) coupled with a Magna-760 spectrometer.

More computer modeling details, including the Cartesian and mol2 type coordinates of various structures, as well as optical microscopic observations of the tubes are reported in the Supporting Information.

Received: June 30, 2003 [Z52259]

Keywords: liquid crystals · nanostructures · nanotubes · peptides · self-assembly

[1] M. R. Ghadiri, J. R. Granja, R. A. Milligan, D. E. McRee, N. Khazanovich, *Nature* **1993**, *366*, 324.
[2] D. T. Bong, T. D. Clark, J. R. Granja, M. R. Ghadiri, *Angew. Chem.* **2001**, *113*, 1016; *Angew. Chem. Int. Ed.* **2001**, *40*, 988; .
[3] D. Ranganathan, C. Lakshimi, I. L. Karle, *J. Am. Chem. Soc.* **1999**, *121*, 6103.
[4] D. Gauthier, P. Baillargeon, M. Drouin, Y. Dory, *Angew. Chem.* **2001**, *113*, 4771; *Angew. Chem. Int. Ed.* **2001**, *40*, 4635.
[5] M. R. Ghadiri, J. R. Granja, L. K. Buehler, *Nature* **1994**, *369*, 301.
[6] G. M. Whitesides, J. P. Mathias, C. T. Seto, *Science* **1991**, *254*, 1312.
[7] a) P. Terech, R. G. Weiss, *Chem. Rev.* **1997**, *97*, 3133; b) C. Geiger, M. Stanescu, L. Chen, D. G. Whitten, *Langmuir* **1999**, *15*, 2241.
[8] a) L. Guan, Y. Zhao, *Chem. Mater.* **2000**, *12*, 3667; b) L. Guan, Y. Zhao, *J. Mater. Chem.* **2001**, *11*, 1339.
[9] P. Meakin, *Adv. Colloid Interface Sci.* **1988**, *28*, 250.
[10] H. Okamoto, T. Nakanishi, Y. Nagai, M. Kasahara, K. Takeda, *J. Am. Chem. Soc.* **2003**, *125*, 2756.
[11] N. Bowden, I. S. Choi, B. A. Grzybowski, G. M. Whitesides, *J. Am. Chem. Soc.* **1999**, *121*, 5373.
[12] T. D. Clark, L. K. Buehler, M. R. Ghadiri, *J. Am. Chem. Soc.* **1998**, *120*, 651.
[13] M. Tsuboi, Y. Kubo, T. Ikeda, S. A. Overman, O. Osman, G. J. Thomas, Jr., *Biochemistry* **2003**, *42*, 940.
[14] M. Tsuboi, F. Kaneuchi, T. Ikeda, K. Akahane, *Can. J. Chem.* **1991**, *69*, 1752.
[15] H.-M. Liem, P. Etchegoin, K. S. Whitehead, D. C. Bradley, *Adv. Mater.* **2003**, *13*, 66.

